

# Bioluminescent Assays for Glucose and Glutamine Metabolism: High-Throughput Screening for Changes in Extracellular and Intracellular Metabolites

SLAS Discovery  
1–12  
© 2016 Society for Laboratory  
Automation and Screening  
DOI: 10.1177/1087057116675612  
jbx.sagepub.com  


Donna Leippe<sup>1</sup>, Mary Sobol<sup>1</sup>, Gediminas Vidugiris<sup>1</sup>,  
James J. Cali<sup>1</sup>, and Jolanta Vidugiriene<sup>1</sup>

## Abstract

Cancer cell metabolism is a complex, dynamic network of regulated pathways. Interrogation of this network would benefit from rapid, sensitive techniques that are adaptable to high-throughput formats, facilitating novel compound screening. This requires assays that have minimal sample preparation and are adaptable to lower-volume 384-well formats and automation. Here we describe bioluminescent glucose, lactate, glutamine, and glutamate detection assays that are well suited for high-throughput analysis of two major metabolic pathways in cancer cells: glycolysis and glutaminolysis. The sensitivity (1–5 pmol/sample), broad linear range (0.1–100  $\mu$ M), and wide dynamic range (>100-fold) are advantageous for measuring both extracellular and intracellular metabolites. Importantly, the assays incorporate rapid inactivation of endogenous enzymes, eliminating deproteinization steps required by other methods. Using ovarian cancer cell lines as a model system, the assays were used to monitor changes in glucose and glutamine consumption and lactate and glutamate secretion over time. Homogeneous formats of the lactate and glutamate assays were robust ( $Z'$  = 0.6–0.9) and could be multiplexed with a real-time viability assay to generate internally controlled data. Screening a small-compound library with these assays resulted in the identification of both inhibitors and activators of lactate and glutamate production.

## Keywords

bioluminescence, cell-based assays, glucose, lactate, glutamine, glutamate, extracellular metabolites

## Introduction

Rapidly proliferating cancer cells need to balance nutrient uptake with energy production, macromolecular biosynthesis, and redox maintenance. Cancer cells adapt by reprogramming metabolic pathways, which then become potential therapeutic targets. These adaptations include increased consumption of glucose for glycolysis and glutamine for glutaminolysis.<sup>1</sup> Aerobic glycolysis is an attractive therapeutic target for inhibiting cancer cell growth.<sup>2</sup> Recent reports that metabolic reprogramming in tumor cells can be disrupted by combined inhibition of glycolysis and mTORC1 signaling create new possibilities for cotargeting metabolic and signaling pathways.<sup>3</sup> In addition, the increase in lactate secretion, once considered a waste product of aerobic glycolysis, has recently emerged as a critical regulator of cancer development and a novel therapeutic target.<sup>4</sup> Glutamine is another abundant and versatile nutrient that has emerged as a central precursor for cancer cell metabolism.<sup>5</sup> In cells, glutamine is converted to glutamate to drive the tricarboxylic acid (TCA) cycle (anaplerosis), to produce glutathione for removing reactive oxygen species, and to serve as a nitrogen

and carbon source for other nonessential amino acids, nucleotides, and fatty acids.<sup>6–8</sup> Many aggressive cancer cells are dependent on glutamine for growth, and increased glutamate secretion is associated with malignant phenotypes.<sup>9</sup>

Glucose and glutamine metabolism are highly interrelated and influenced by multiple oncogenic signaling pathways. For example, glutamine transport is the rate-limiting step in mTOR activation, whereas glucose transport is up-regulated by mTOR.<sup>10,11</sup> c-Myc is another oncogene that has several roles in tumor cell metabolism.<sup>6</sup> The expression of genes involved in glutamine metabolism, such as

<sup>1</sup>Research and Development, Promega Corporation, Madison, WI, USA

Received Jul 1, 2016, and in revised form Sep 7, 2016. Accepted for publication Sep 27, 2016.

Supplementary material for this article is available on the *Journal of Biomolecular Screening* Web site at <http://jbx.sagepub.com/supplemental>.

## Corresponding Author:

Jolanta Vidugiriene, Research and Development, Promega Corporation, Madison, WI, USA.

Email: [jolanta.vidugiriene@promega.com](mailto:jolanta.vidugiriene@promega.com)

glutamine transporter and glutaminase, is induced by c-Myc, and cells overexpressing c-Myc are particularly sensitive to glutamine deprivation.<sup>12,13</sup>

Methods used to study glucose and glutamine metabolism include analytical methods (mass spectrometry, liquid chromatography/mass spectrometry, nuclear magnetic resonance) for metabolite profiling, stable isotope labeling for tracking metabolites, and colorimetric or fluorometric enzymatic assays and various bioanalyzers for measuring changes in metabolite levels.<sup>14–17</sup>

Metabolic profiling enables systemwide measurements of hundreds of metabolites, revealing distinct metabolic signatures of cancer cells in a single experiment.<sup>18</sup> Stable isotope labeling follows the fate of labeled metabolites and has been used to establish the contribution of glucose and glutamine carbon atoms to the well-defined pathways of central carbon metabolism including glycolysis, the pentose phosphate pathway, and the TCA cycle.<sup>14</sup> Both approaches provide comprehensive information about the changes of multiple metabolites under specific experimental conditions, but they require extensive sample preparation and are not designed or well suited for looking at select key metabolites under multiple treatment conditions, for example, screening a small-molecule library.

Bioanalyzers can be used for detecting extracellular levels of glucose, lactate, glutamine, and glutamate and are primarily based on enzymatic technology using metabolite-selective oxidases. The amount of sample needed can be large, and throughput is limited. Colorimetric and fluorometric detection assays use metabolite-selective oxidases or dehydrogenases coupled to hydrogen peroxide or NAD(P)H detection, respectively. These assays can be used for measuring metabolite changes in cell lysates and are often used for measuring changes in extracellular glucose and lactate levels<sup>15</sup>; however, centrifugation and deproteinization steps make the assays cumbersome for high-throughput applications.

The increasing interest in glucose and glutamine metabolism and its interaction with oncogenic signaling pathways makes a method for high-throughput analysis of changes in cellular glucose, lactate, glutamine, and glutamate very beneficial. Such high-throughput screening (HTS) can not only help reveal novel inhibitors of glucose and glutamine-dependent metabolic pathways but can also uncover yet unidentified links between metabolic and signaling pathways. Recently, HTS with breast cancer cell lines identified potent inhibitors of glutamate secretion that may lead to novel approaches for treating cancer pain.<sup>19</sup> However, because of the lack of HTS tools, information for using HTS to evaluate the effects of small molecules on major metabolic pathways is limited.

To address this need, we evaluated the applicability of bioluminescent glucose, lactate, glutamine, and glutamate assays for HTS. As a model system, we used two ovarian

cancer cell lines shown to have different glutamine dependencies. OVCAR-3 cells are low invasive and glutamine independent, whereas SKOV-3 cells are high invasive and require glutamine for growth.<sup>9</sup> The four assays detected changes in the levels of metabolites in cell culture medium, could be performed in 384-well plates, and had  $Z'$  values<sup>20</sup> suitable for screening. To measure changes in extracellular metabolite levels over time, a small amount of culture medium was collected and used to measure all four metabolites. We also developed a homogeneous assay format to measure the production of lactate and glutamate. Using the Library of Pharmacologically Active Compounds (LOPAC<sup>1280</sup>; Sigma Aldrich, St. Louis, MO) as a model library, compounds that altered the production of lactate and glutamate by SKOV-3 cells were identified. These results demonstrate the robustness of the assays for high-throughput studies and identification of novel inhibitors or activators for two major metabolic pathways in cancer: glycolysis and glutaminolysis.

## Materials and Methods

### Cell Culture

SKOV-3 and OVCAR-3 ovarian cancer cell lines were obtained from ATCC (Manassas, VA). SKOV-3 cells (ATCC HTB-77) were cultured in McCoy's 5A medium (Gibco, ThermoFisher Scientific, Waltham, MA). OVCAR-3 cells (ATCC HTB-161) were cultured in RPMI 1640 medium (Gibco) supplemented with 10  $\mu$ g/mL insulin (Sigma). Growth media were supplemented with 10% fetal bovine serum (FBS; Gibco). The concentration of glucose, lactate, and other components in medium and serum can influence the rate of metabolic pathways. To control these concentrations, glucose- and glutamine-free DMEM (Gibco No. A14430-01) was used. Before experiments, glucose (Gibco) and glutamine (ATCC) were added to the DMEM such that the final concentrations were 5 mM and 2 mM, respectively. When indicated, DMEM was supplemented with 10% dialyzed FBS (Gibco No. 26400).

### Metabolite Detection Assay Protocol and Standard Curves

The metabolite detection assays were developed using a previously described bioluminescent NADH detection technology consisting of diaphorase enzyme, pro-luciferin diaphorase substrate, adenosine triphosphate, and luciferase.<sup>21,22</sup> Each metabolite detection reagent contained these components in a luciferin detection buffer with NAD and a selective dehydrogenase. The dehydrogenases and their concentrations in the detection reagents were lactate dehydrogenase (5 u/mL, No. 427217, EMD Millipore, Billerica, MA), glutamate dehydrogenase (20 u/mL, No. 10197734001, Sigma) and

glucose dehydrogenase (40 u/mL, No. DG1003, Gojira Fine Chemicals, Bedford Heights, OH). The detection reagents contained all components necessary to measure glucose, lactate, or glutamate and were added directly to the samples at a 1:1 ratio. For glutamine detection, it was first necessary to use glutaminase to convert glutamine to glutamate before adding the glutamate detection reagent. For glucose, lactate, and glutamate, the light output was directly proportional to the amount of metabolite in the sample. However, the amount of glutamine in a sample was calculated by subtracting the signal in the absence of glutaminase from the signal in the presence of glutaminase.

The performance of each metabolite detection assay was characterized using glucose, lactate, glutamine, and glutamate standards serially diluted in phosphate-buffered saline (PBS). Nine microliters of glucose and lactate standards were transferred into 384-well low-volume (LV) plates and 9  $\mu$ L of glucose or lactate detection reagent was added, respectively, to start the reaction. For glutamine and glutamate, 4.5  $\mu$ L of standards were transferred into 384-well LV plates, and 4.5  $\mu$ L of glutaminase buffer (100 mM sodium acetate pH 5.2) with glutaminase (for glutamine, Gojira No. GL1008, 0.5 u/mL) or without glutaminase (for glutamate) was added. The glutaminase reaction continued for 30 min at room temperature (RT), after which 9  $\mu$ L of glutamate detection reagent was added to both samples. All reactions were then incubated for 1 h at RT, and luminescence was recorded using an Infinite M1000 Pro plate reader (Tecan, Männedorf, Switzerland). The data are presented in figures as average relative light units (RLU) of quadruplicate reactions.

### Detection of Intracellular Metabolites in Cell Lysates

For measuring intracellular metabolite levels, OVCAR-3 and SKOV-3 cells were trypsinized, collected, and, after a quick wash with cold PBS, resuspended in 0.5 mL PBS at  $2.2 \times 10^6$  cells/mL. The cells were rapidly lysed by adding 0.25 mL of 0.6N HCl/0.1% dodecyltrimethyl ammonium bromide (DTAB; Sigma No. D8638). The samples were neutralized with 0.25 mL of 1 M Trizma (Sigma) and were serially diluted twofold in a solution of premixed 0.5 mL PBS, 0.25 mL 0.6N HCl/0.1% DTAB, 0.25 mL Trizma. For glutamine and glutamate analysis, the acid and base were 0.3 N HCl/0.1% DTAB and 450 mM Tris pH 8.0. Cell lysates were transferred into 384-well LV plates (9  $\mu$ L for lactate and glucose and 4.5  $\mu$ L for glutamine and glutamate) and assayed following the protocol described above.

For spike recovery experiments, known concentrations of glucose, lactate, glutamate, and glutamine were added to cells in PBS or to PBS alone. The samples were then lysed and processed as described above. The percentage recoveries of spiked metabolites were calculated using the equation

$$\% \text{ Recovery} = 100 \times ((\text{RLU spike in cells} - \text{RLU cells}) / \text{RLU spike in PBS alone}).$$

Concentrations of glucose, lactate, glutamine, and glutamate in cell lysates were calculated from standard curves assayed in the same plates using the same experimental conditions as the cell lysate samples. Intracellular metabolite concentrations were calculated using the number of lysed cells per well and assuming a mammalian cell intracellular volume of  $\sim 2.5$  pL as reported for HeLa cells.<sup>23</sup>

### Detection of Extracellular Metabolites in Medium

For measuring changes in glucose, lactate, glutamine, and glutamate in medium, SKOV-3 and OVCAR-3 cells were plated in 384-well tissue culture-treated plates at different cell densities in 80  $\mu$ L DMEM medium supplemented with 5 mM glucose, 2 mM glutamine, and 10% dialyzed FBS. The cells were incubated in a tissue culture incubator (37 °C, 5% CO<sub>2</sub>). At indicated time points (24, 48, 72 h), 2  $\mu$ L of medium was removed and transferred to separate 96-well plates containing 98  $\mu$ L PBS/well. The diluted medium samples were stored frozen at  $-20$  °C until all the samples were collected. For metabolite analysis, 9  $\mu$ L of thawed sample was transferred to wells of 384-well LV plates for lactate detection, and 4.5  $\mu$ L was transferred for glucose, glutamine, and glutamate detection. An additional 4.5  $\mu$ L PBS was added to the glucose samples to fit into the linear range of the assay. Samples were then assayed as described above.

For measuring Z', the medium was collected using a 96-tip semiautomated 20  $\mu$ L BenchTop Pipettor (Sorenson BioScience, Salt Lake City, UT). For the metabolite analysis, the samples and the reagents were dispensed into 384-well LV plates using a Multidrop Combi\_nL Reagent Dispenser (Multidrop; ThermoFisher Scientific). Luminescence was read using an Infinite M200 plate reader (Tecan).

### Homogenous Detection of Lactate and Glutamate in Medium

A homogenous assay format was developed for measuring lactate and glutamate production by OVCAR-3 and SKOV-3 cells. OVCAR-3 or SKOV-3 cells were prepared in DMEM medium containing RealTime-Glo MT Cell Viability Assay reagents (Promega, Madison, WI). This real-time viability assay allows continuous monitoring of cell viability by luminescence.<sup>24</sup> The cells or medium alone was dispensed into 384-well LV plates at 4  $\mu$ L/well. Lactate and glutamate production was started by adding 2  $\mu$ L of medium containing 15 mM glucose and 6 mM glutamine. The cells were incubated at 37 °C in a tissue culture incubator. To determine optimal conditions for HTS screening, the experiments were performed at three cell densities (2.5 K, 1.5 K, and 1 K per well), and lactate

and glutamate production was measured at three time points (0.5, 1, and 2 h after adding glucose and glutamine). At each time point, the plates were removed from the incubator, and luminescence from the viability assay was read to record any changes in viability. After reading the plate, the lactate and glutamate secretion was stopped by adding 2  $\mu$ L of 0.3 N HCl/0.1% DTAB to lyse cells and fix metabolite concentrations. The lysis solution also terminates viability assay luminescence. The plates were held at RT until all samples were collected. The metabolite detection reactions were started by addition of 9  $\mu$ L of lactate or glutamate detection reagent premixed with 1 M Trizma. (The detection reagent and Trizma were premixed by adding eight volumes of detection reagent to one volume of Trizma.) Luminescence was read after a 1 h incubation at RT. All the reagents were dispensed using a Multidrop, except for the corrosive 0.3 N HCl/0.1% DTAB solution, which was dispensed with a Mantis liquid handler (Formulatrix, Bedford, MA).

### LOPAC Library Screening

The LOPAC is a collection of 1280 pharmacologically active compounds from 56 pharmacological classes (Sigma, No. LO4100). For the screening assays, 5 nL of 10 mM compound in DMSO stocks were dispensed into 384-well LV plates using an ECHO 555 acoustic liquid handler (LabCyte, Sunnyvale, CA). Each compound was dispensed in quadruplicate wells. Next, 6  $\mu$ L of SKOV-3 cells resuspended in unsupplemented DMEM containing real-time viability reagents was dispensed at 1000 cells/well using a Multidrop. Medium containing 0.1% DMSO with and without cells was used for vehicle-matched positive and negative controls in columns 1, 2, 23, and 24, rows A–H and I–P, respectively. There were 32 positive control wells containing untreated cells and 32 negative control wells containing medium only per plate. After 15 min preincubation at RT ( $\sim$ 23  $^{\circ}$ C), 2  $\mu$ L of medium containing 20 mM glucose and 8 mM glutamine was added to all samples, and the plates were placed in a tissue culture incubator (37  $^{\circ}$ C, 5% CO<sub>2</sub>). After 1 h incubation, luminescence was measured using an Infinite M200 plate reader to determine changes in viability. Immediately after viability measurements, 1  $\mu$ L 0.6 N HCl/0.1% DTAB was added to each sample using the Mantis dispenser. The plates were kept at RT until all the plates were processed. To start lactate and glutamate detection, 9  $\mu$ L of lactate or glutamate detection reagent premixed with 1 M Trizma (at an 8:1 ratio) was added to the plates. The plates were incubated for 90 min at RT and luminescence was measured. After the 90 min incubation, all the lactate and glutamate has been converted to light and the luminescent signal reaches steady state, making the assays suitable for batch processing. This screening protocol is outlined in **Supplemental Table S2**.

### Hit Characterization

The most potent hits identified by screening were further studied using concentration-response curves. When commercially available, compounds were purchased to prepare fresh 10 mM stock solutions in DMSO. Otherwise, samples of the original library 10 mM stock solutions in DMSO were used. The 10 mM compound stocks were diluted to 300  $\mu$ M in DMEM (final concentration 3% DMSO). Serial twofold dilutions were prepared in DMEM plus 3% DMSO. Ten microliters were added to quadruplicate wells in a 384-well plate. Fifteen microliters of SKOV-3 cells (4000 cells/well) in DMEM with 2 $\times$  real-time viability reagents were added and preincubated with compound for 15 min at RT. Five microliters of DMEM containing 30 mM glucose and 12 mM glutamine were added, and the plates were placed in a 37  $^{\circ}$ C tissue culture incubator for 1 h. At the end of the incubation, viability luminescence was measured before lysing the cells and stopping metabolite production with 5  $\mu$ L of 0.6 N HCl/0.1% DTAB. Glutamate or lactate was detected using 45  $\mu$ L of the appropriate detection reagent premixed with 1 M Trizma (8:1 volume reagent to volume Trizma). The plates were incubated for 60 to 90 min at RT before luminescence was measured.

Counterscreening assays using glutamate or lactate standards were used to identify compounds that interfered with the detection system and were false hits. In these assays, instead of cells, 15  $\mu$ L of 40  $\mu$ M lactate or 40  $\mu$ M glutamate controls were added to wells containing compound and then assayed as above.

### Data Analysis and Statistical Validation for HTS Applications

The robustness of the assays for HTS applications was evaluated by determining signal-to-background (S/B), signal-to-noise (S/N), and  $Z'$ . S/B was calculated by dividing the mean signal from samples by the mean signal from negative controls. For some experiments, in which negative control signal was higher than the signal from samples, an analogous high signal-to-low signal ratio was calculated. S/N was calculated by dividing the net signal (mean signal minus mean negative control) by the standard deviation of the negative control.  $Z'$  factor<sup>20</sup> was calculated as follows:  $Z' = 1 - ((3 \times \text{St.Dev. of High Signal} + 3 \times \text{St.Dev. of Low Signal}) / \text{Mean of High Signal} - \text{Mean of Low Signal})$ .

## Results

### Characterization of the Bioluminescent Metabolite Assays

The lactate, glucose, and glutamate metabolite detection assays use metabolite-selective dehydrogenases coupled to

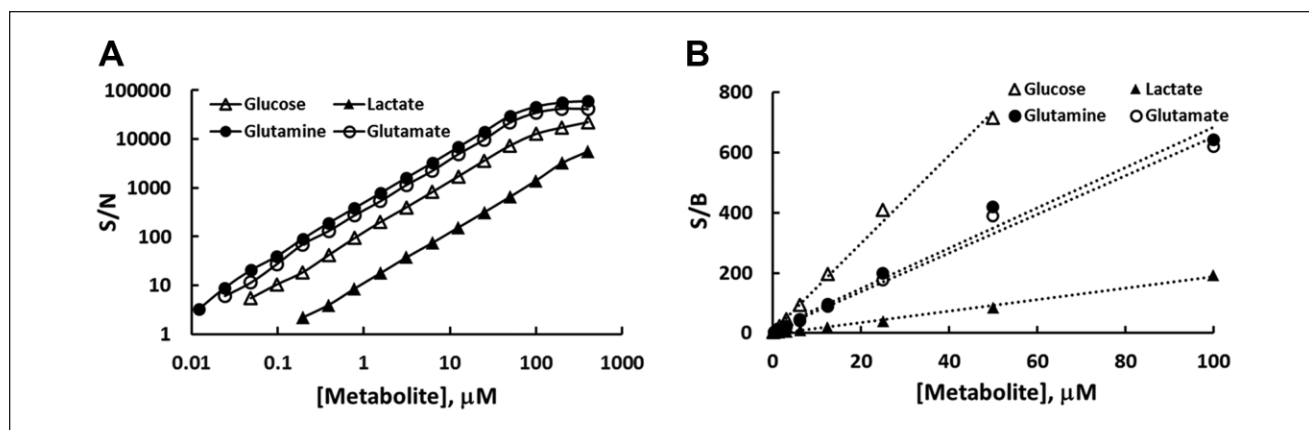


**Figure 1.** Assay characterization. Sensitivity, linear range, and assay window were determined for each assay. Standard curves were generated using twofold serial dilutions of lactate, glucose, glutamine, and glutamate in phosphate-buffered saline. Dilutions were assayed in quadruplicate using the protocols described in the Materials and Methods section. Luminescence was recorded after a 60 min incubation. The average signal was used to calculate S/N (A) and S/B (B) ratios.

a previously described bioluminescent NAD(P)H detection technology.<sup>21,22</sup> Each dehydrogenase produces NADH in proportion to the amount of analyte present in a sample. The NADH detection technology uses a reductase enzyme and a proluciferin substrate in combination with a luciferase enzyme to produce a light signal that is proportional to the starting amount of NADH and therefore the starting amount of metabolite. For measuring glucose and lactate, the detection reagents contain all components necessary to measure the metabolite and are added directly to the samples at a 1:1 ratio. For glutamine and glutamate detection, the samples are split and treated with and without glutaminase (to convert glutamine to glutamate), and then glutamate detection reagent is added to both samples at a 1:1 ratio. The amount of glutamine present in the samples is detected as the difference between the light signals of the two samples.

To determine the sensitivity, linearity, and assay window of each detection assay, we prepared a metabolite titration curve in 384-well LV plates and assayed the metabolite with the appropriate detection reagent. Luminescence was recorded (Suppl. Table S1), and the assay sensitivity and window were determined by calculating S/N and S/B ratios. As shown in Figure 1, the sensitivity of each assay was in the nanomolar range, with the limit of detection (defined as S/N = 3) of ~400 nM (3.6 pmol/9 μL) for lactate and ~100 nM (0.9 pmol/9 μL) for glucose, glutamine, and glutamate. All assays had wide linear ranges (~3 logs) with maximum S/B ratios ranging from ~120 for lactate to more than 500 for glucose, glutamine, and glutamate.

### Intracellular Metabolite Levels

We next determined the ability of the assays to detect intracellular metabolite levels. We used two ovarian cancer cell lines, SKOV-3 and OVCAR-3, known to have different

glutamine dependencies.<sup>9</sup> Cell lysates were prepared from both cell lines, serially diluted twofold, and assayed in 384-well LV plates. Endogenous dehydrogenases and reduced dinucleotides (NADH/NADPH) have direct effects on metabolite detection assays, so typically, sample deproteinization and degradation of reduced dinucleotides are required before measurements. To incorporate a sample preparation step that is also HTS compatible, we used a strong acid/detergent mixture to prepare the cell lysates as well as rapidly inactivate endogenous enzymes and simultaneously degrade endogenous NAD(P)H. To confirm the effectiveness of this approach, we added the detection system without metabolite-selective dehydrogenases to cell lysates and saw no significant light increase compared with a no-cell control (data not shown). In the presence of metabolite-selective dehydrogenases, a linear increase in light output with increasing number of OVCAR-3 cells was observed for all four metabolites (Suppl. Fig. S1). The limit of detection (at S/N = 3) depended on the intracellular metabolite levels as well as assay sensitivity and ranged from ~650 cells/well for lactate and glucose and ~10 cells/well for glutamine and glutamate. The signals were linear up to 10,000 cell/well (Suppl. Fig. S1). The quantitative and specific detection of cellular metabolites was further confirmed using a spike-recovery experiment. Addition of a known concentration of metabolite to cells before cell lysis resulted in 84% spike recovery for lactate and higher recoveries for the other metabolites (Suppl. Fig. S2).

When intracellular amounts of metabolites were compared between OVCAR-3 and SKOV-3 cells, the lactate and glucose levels were similar; however, a significant difference was observed in glutamine and glutamate concentrations (Fig. 2A,B). For example, 2500 OVCAR-3 or SKOV-3 cell equivalents in 9 μL had ~9.7 μM (87 pmol per well) lactate, indicating the intracellular concentration of lactate in

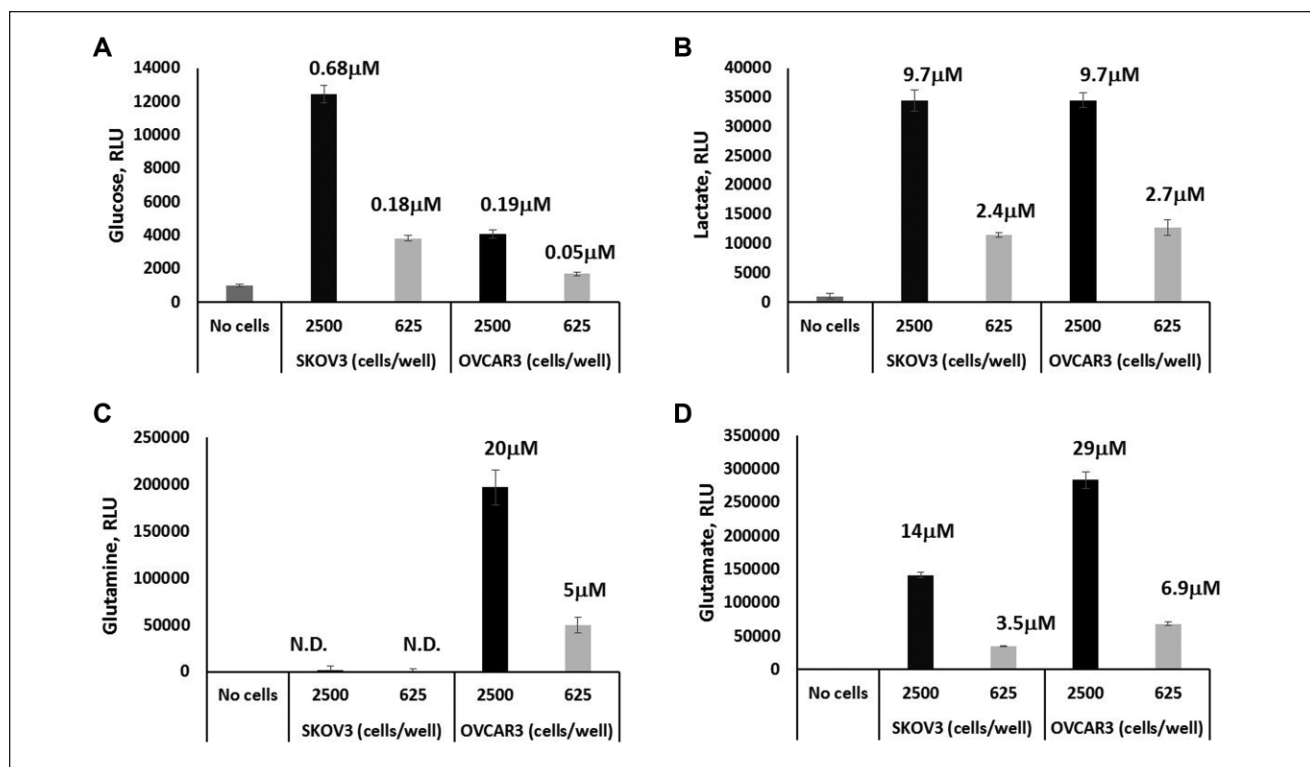


**Figure 2.** Metabolite detection in cell lysates. SKOV-3 and OVCAR-3 cells were collected and lysed as described in the Materials and Methods section. The cell lysates were titrated and then used to measure all four metabolites in eight replicate wells. The mean relative light units (RLU) are shown for glucose (A), lactate (B), glutamine (C), and glutamate (D) detection using 2500 cells/well (black bars), 625 cells/well (light bars), and no cell controls (dark gray bars). The values above the bars are the calculated concentration of each metabolite in 9  $\mu\text{L}$  of lysate from the indicated amount of cells/well. Error bars are  $\pm 1$  SD.

both cell lines is  $\sim 14$  mM (calculated using a cell volume of  $\sim 2.5$  pL<sup>23</sup>). Upon uptake into cells, glucose is rapidly phosphorylated by hexokinase, and therefore the concentration of glucose in both cell lysates was low, ranging from 0.19  $\mu\text{M}$  for OVCAR-3 to 0.68  $\mu\text{M}$  for SKOV-3, corresponding to intracellular levels of 0.25 mM and 0.9 mM, respectively. Glutamine was the most significantly different metabolite between the two cell lines. In SKOV-3 lysates, glutamine was not detected with significance, whereas OVCAR-3 lysates had 20  $\mu\text{M}$  glutamine, equal to 28 mM intracellular glutamine (Fig. 2C). Although the amount of glutamine greatly differed between the two cell lines, both contained significant amounts of glutamate (Fig. 2D). The calculated intracellular concentrations of glutamate were 20 mM for SKOV-3 and 41 mM for OVCAR-3.

### Changes in Extracellular Metabolites over Time

To further characterize the metabolic profiles of OVCAR-3 and SKOV-3 cells, changes in extracellular metabolite levels during growth in culture were measured. The starting concentrations of glucose and glutamine in culture medium are in the millimolar range, and as cells grow and consume these metabolites, concentrations decrease significantly (>50-fold).

During growth, lactate and glutamate are secreted and accumulate in medium, reaching millimolar levels in 48 to 72 h. To measure these concentration changes, medium samples typically require dilution into the linear range of an assay, and different dilutions might be needed for different metabolites and for early and late time points. However, the bioluminescent assays have broad linear ranges (Fig. 1) that could accommodate the full range of expected concentrations with a single dilution factor. To confirm this, SKOV-3 and OVCAR-3 cells were plated at different densities in 384-well plates in DMEM containing 5 mM glucose, 2 mM glutamine, and 10% dialyzed serum. Medium samples were collected at 24, 48, and 72 h time points; diluted 50-fold; and stored frozen until analysis. For metabolite detection, part of the thawed sample was transferred into 384-well LV plates, and the appropriate metabolite detection reagent was added to the samples. All four metabolites were measured from the same set of diluted samples. Assay robustness required for HTS was also determined by calculating  $Z'$  values.<sup>20</sup>

As shown in Figure 3, the cells consumed glucose and glutamine and secreted lactate and glutamate with time and cell density dependence. Glucose and glutamine consumption were more robust at greater cell densities and longer incubation times ( $Z' \geq 6$ ; Suppl. Table S3). In contrast, lactate and

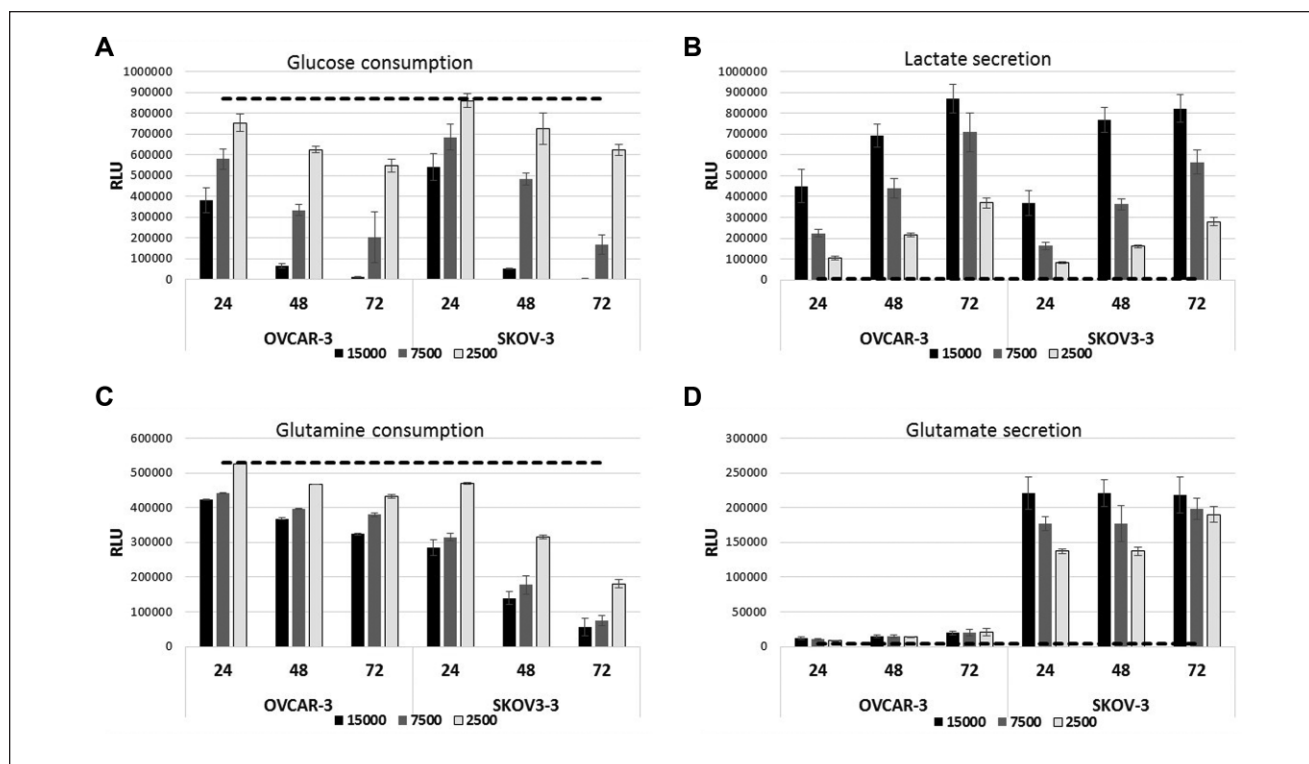


**Figure 3.** Changes in metabolite levels in culture media during cell growth. OVCAR-3 and SKOV-3 cells were plated at 2500 (light gray bars), 7500 (dark gray bars), and 15,000 (black bars) cells/well in 80  $\mu$ L in 384-well plates. At 24, 48, and 72 h, 2  $\mu$ L of media was removed, diluted into 98  $\mu$ L of PBS, and stored frozen. The samples were then thawed and assayed in 384-well LV plates to determine the levels of glucose (A), lactate (B), glutamine (C), and glutamate (D). Medium without cells was used as a negative control and is represented as dashed lines. Each data point represents the mean of eight replicates. Error bars are  $\pm$  1 SD.

glutamate secretion were robustly detected at all cell densities and time points ( $Z' \geq 6$ ; **Suppl. Table S3**).

The kinetic data clearly revealed distinct metabolic profiles of the two ovarian cancer cell lines. Both cell lines consumed glucose and secreted lactate at comparable rates (**Fig. 3A,B**). After 72 h, both cell lines consumed more than 90% of the glucose ( $>4.5$  mM) and secreted about 8 mM lactate at the highest cell density. The lactate/glucose ratio was  $\sim 1.7$  for both cell lines. However, glutamine metabolism was significantly different in OVCAR-3 and SKOV-3 cells (**Fig. 3C,D**). SKOV-3 cells consumed more than 90% ( $\sim 1.8$  mM) of the glutamine in comparison to  $\sim 75\%$  ( $\sim 1.5$  mM) by OVCAR-3 cells, and glutamate secretion revealed an even greater difference: SKOV-3 cells secreted 20 times more glutamate than OVCAR-3 cells ( $\sim 0.7$  mM compared with 0.03 mM) with a glutamate secretion/glutamine consumption ratio of  $\sim 0.38$  for SKOV-3 cells and 0.02 for OVCAR-3 cells.

### Homogeneous Assay Format for Lactate and Glutamate Production

In the above experiment, extracellular metabolites were measured in samples of medium collected 24 h after plating.

We also wanted to develop an assay format that was homogeneous, capable of assaying medium directly in the wells of cells without medium removal and dilution steps. This format measures total metabolite levels in the well (extracellular plus intracellular levels), which have to be within the linear range of the detection assay. The method also needs a step for rapid cell lysis and inactivation of endogenous enzymes. We focused on the lactate and glutamate assays because of the low rates of change in glucose and glutamine levels prior to 24 h. To determine if the bioluminescent lactate and glutamate detection assays could meet these criteria, OVCAR-3 and SKOV-3 cells were plated at three densities (2.5 K, 1.5 K, and 1 K cells/well) and analyzed at three time points (0.5, 1, and 2 h). Under all conditions, lactate concentration (intracellular plus secreted lactate) was within the linear range of the assay with  $Z' > 0.5$ . Data and  $Z'$  values for 1000 SKOV-3 cells analyzed at 1 h are shown in **Figure 4B** (data not shown for other conditions). Glutamate secretion by SKOV-3 cells exceeded the linear range at high cell density or long incubation time, and at low cell density or short incubation time, the assay window was not sufficient to measure glutamate secretion by OVCAR-3 cells (data not shown). However, conditions could be established that provided robust performance with both cell lines: the 1 h time

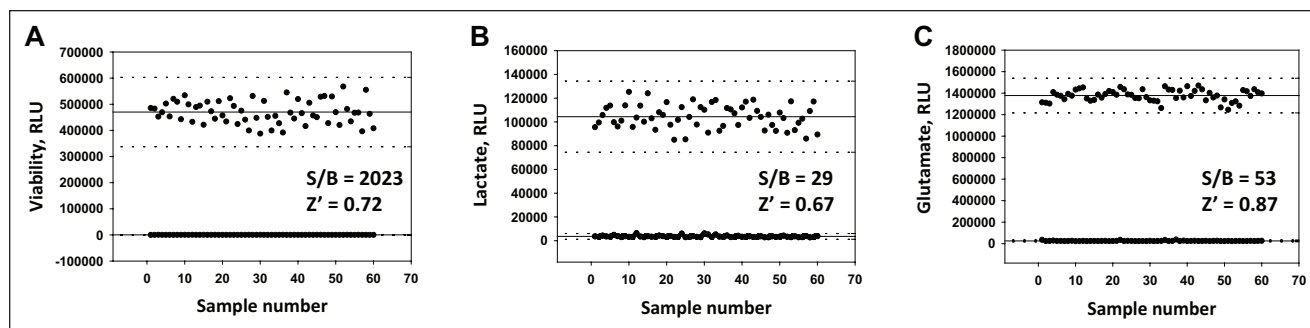


**Figure 4.**  $Z'$  factor estimation for the homogeneous assay format. SKOV-3 cells were added to 60 wells in each of two 384-well low-volume plates. Each well contained 1000 cells in 6  $\mu$ L DMEM containing 5 mM glucose and 2 mM glutamine. Medium without cells was used for controls. After a 1 h incubation at 37 °C in a tissue culture incubator, the plates were removed and the viability measured. The cells were then lysed, and the samples were assayed for lactate or glutamate using the protocol for the homogeneous format. Relative light units measured from each well are plotted for the viability assay, using the lactate assay plate (**A**), lactate assay (**B**), and glutamate assay (**C**). The signal-to-background ratio and  $Z'$  value were calculated using wells with medium only as the low-signal control. The dashed lines represent  $\pm 3$  SD from the mean signal.

point using 2500 OVCAR-3 cells or 1000 SKOV-3 cells (**Fig. 4C**, data not shown for OVCAR-3 cells). We incorporated viability measurements in the homogeneous assay workflow using a real-time viability assay described in the Materials and Methods section. When added to live metabolically active cells, this assay produces a luminescent signal that is quenched when cells are lysed.<sup>24</sup> This feature allows it to be multiplexed with the metabolite detection to provide internally controlled data from the same set of wells. Viability readings, taken before cell lysis, from all assays were similar, and representative data for SKOV-3 cells are in **Figure 4A**.

The homogeneous assays were validated using known inhibitors of glycolysis and glutaminase. Incubation of cells with the glycolysis inhibitor 2-deoxy-D-glucose decreased lactate levels, whereas the glutaminase inhibitor BPTES reduced glutamate amounts (**Suppl. Fig. S3**). Concentrations of inhibitors needed to reduce metabolite levels to  $\sim 40\%$  of controls did not affect cell viability or the detection systems.

### Library Screening

To further evaluate the utility of bioluminescent lactate and glutamate detection assays for HTS applications, we screened a small-molecule library for compounds that might increase or decrease lactate and/or glutamate production. We chose to screen the commercially available LOPAC collection of 1280 small compounds using the homogeneous lactate and glutamate assays. The library was screened with SKOV-3 cells at 1000 cells/well with 1 h incubation, conditions previously identified as optimal for both lactate and glutamate detection (**Fig. 4**). Two separate sets of the library compounds dispensed in quadruplicate wells were used to screen the two assays. For each screen, the metabolite detection assays were multiplexed

with the luminescent viability assay. Calculated  $Z'$  factors for the screens ranged from 0.69 to 0.83 for viability, 0.62 to 0.78 for lactate, and 0.62 to 0.73 for glutamate assays (**Suppl. Fig. S4**). For data analysis, RLUs were converted into percentages of positive control wells (untreated cells) on each plate and were calculated for each individual assay. **Figure 5A,B** shows the responses of library compounds ordered from lowest to highest percentage of control for each assay. With both assays, compounds were identified that had lower than control and higher than control signals. The compounds were also grouped according to pharmacological class designation, and responses were not confined to any one class (**Suppl. Fig. S5**).

The hit limit, defined as three standard deviations from the mean control value, corresponded to  $\sim 25\%$  for both assays. Ninety-two compounds in the lactate assay and 66 compounds in the glutamate assay showed  $>25\%$  inhibition or  $>125\%$  activation, corresponding to hit rates of 7.2% and 5.1%, respectively. After eliminating compounds that decreased cell viability by  $>25\%$  from further analysis, lactate and glutamate assay values from each well were normalized to viability readings and percentage inhibition or activation calculated. The normalized data are shown in **Figure 5C,D**.

Thirteen hits for lactate and nine hits for glutamate were among the most potent hits with  $>50\%$  inhibition or  $>150\%$  activation (**Fig. 5C,D**). These most active hits were selected for further analysis in concentration-response experiments with cells. They were also counter-screened with lactate or glutamate controls to determine if any directly affected the detection system. The 13 hits identified for lactate production included two inhibitors and 11 activators (**Fig. 5C**). Both of the inhibitors and three of the activators strongly affected the detection system and were considered false-positive hits (data not

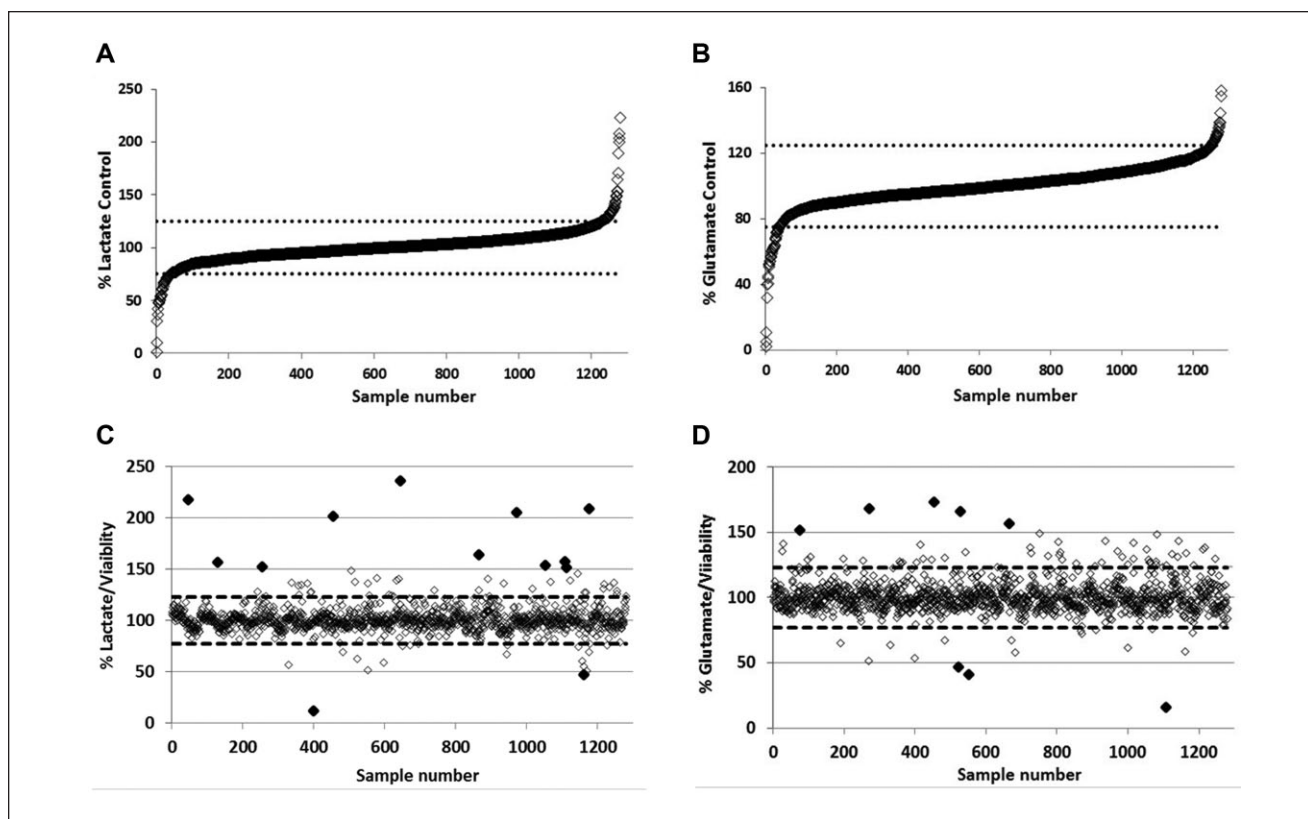


**Figure 5.** LOPAC screening using homogeneous lactate and glutamate detection assays. Two sets of the LOPAC library were used for screening with SKOV-3 cells, one for each assay, as described in the Materials and Methods section. (**A, B**) Plot of hits from lowest to highest percentage control for lactate (**A**) and glutamate (**B**). Each compound was screened in quadruplicate, and the relative light units (RLU) values were averaged. To calculate percentage control, the average RLU was divided by the average of the control wells on each plate. Dashed lines represent three standard deviations from the mean for each assay,  $\sim\pm 25\%$ . (**C, D**) Graph of percentage control normalized to same-well viability measurements for lactate (**C**) and glutamate (**D**). The compounds are ordered according to library number. The RLU value of each well was normalized to the same-well viability reading before dividing by control values. Dashed lines represent three standard deviations from the mean for each assay,  $\sim\pm 25\%$ . Two of the compounds with  $>150\%$  activity for glutamate, Nos. 666 and 668, are overlapping in this plot.

shown). When tested, one of the remaining eight activators, compound 1112, showed concentration-dependent increases in lactate production (data not shown). Compound 1112 (Sigma Cat. No. R8875) is rotenone, an inhibitor of mitochondrial complex I known to quickly increase lactate secretion.<sup>25</sup> Nine library compounds altered glutamate production, three inhibitors and six activators (**Fig. 5D**). One of the inhibitors was found to affect the detection system such that changes in glutamate production could not be determined (data not shown). Another inhibitor, compound 1108, was determined to be a positive hit (**Fig. 6A**). Although compound 1108 decreased viability at higher concentrations ( $\geq 10 \mu\text{M}$ ), inhibition of glutamate production was seen at much lower doses (at 0.1 to 1  $\mu\text{M}$ ). Among the activators, one compound, 530, was confirmed to be a positive hit, increasing production of glutamate without affecting the detection system (**Fig. 6B**).

## Discussion

There is growing interest in developing therapies that target the altered metabolism of cancer cells. Differences in metabolic profiles of poorly and highly aggressive, glutamine-independent and -dependent tumors have raised the possibility that multiple, separate metabolic pathways will need to be targeted even within the same tumor type.<sup>9</sup> Studies with panels of cancer cell lines, such as ovarian, breast, and kidney, have reported differences in glutamine metabolism that correlate with tumor grade and invasiveness<sup>9,26</sup> and subtype and inhibitor responsiveness.<sup>27</sup> Analysis of metabolic pathways in higher-throughput formats might facilitate a deeper understanding of these phenotypes by uncovering underlying regulatory processes, including ones that may distinguish between different cell phenotypes. Methods such as metabolomics approaches provide a snapshot of many metabolites but only under a limited number of treatment

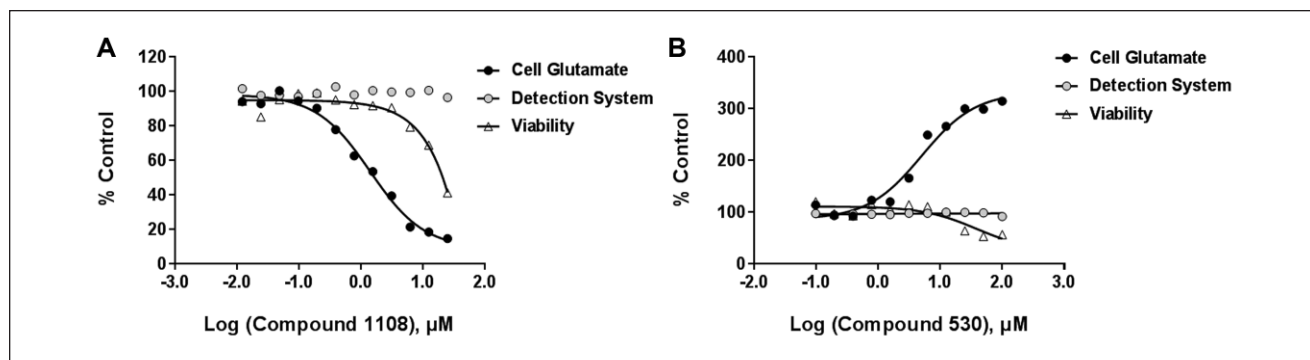


**Figure 6.** Compounds that inhibit or activate metabolite production. Compounds that scored as hits were further tested in concentration-response experiments using twofold dilutions of compounds. The effects of compounds on cell metabolite production and viability were determined, from the same wells, using the homogeneous assay format as described in the Materials and Methods section. Compounds were also analyzed for effects on the detection system using metabolite controls. All concentrations were assayed in quadruplicate. The concentrations plotted on the x-axis are the concentrations in the 30  $\mu\text{L}$  reaction with cells or metabolite. Average relative light units were calculated and divided by signals from negative controls that received no compound. The results are plotted as percentage control. **(A)** Results for compound 1108, which was confirmed to inhibit glutamate production by cells (compound 1108, Sigma S5890, sanguinarine chloride). **(B)** Results for compound 503, which was confirmed to activate glutamate production by cells (compound 503, Sigma G6793, GW7647).

conditions. They are not designed for studying several variables, such as small molecules or other modulators, in high-throughput applications.

In this report, metabolite detection assays developed to measure glucose, lactate, glutamate, and glutamine were characterized and evaluated for adaptability to HTS. The core bioluminescent NADH detection technology in these assays has been successfully used to measure intracellular NAD and NADH in high-throughput applications.<sup>22,28</sup> The metabolite detection assays were sensitive, had wide linear ranges, and had large assay windows, features that gave the assays flexibility and are necessary for HTS. They were used to measure intracellular, extracellular, and, in a homogeneous format, total (intracellular plus extracellular) metabolites.

Intracellular levels of metabolites were detected with high sensitivity (with  $\sim 10$  to 650 cells/well). The concentrations we obtained were within the range of those reported in the literature.<sup>29</sup> However, because intracellular levels vary with cell type and growth conditions and can change rapidly during sampling handling, correlating values obtained using different methods can be challenging. We observed a difference in glutamine metabolism between OVCAR-3 and SKOV-3 cells, confirming what has been reported in the literature.<sup>9</sup> Glutamine was measurable in OVCAR-3 cells but was present at low levels in SKOV-3 cells and could be detected only with higher numbers of cells (data not shown). With lower cell numbers, we cannot exclude the possibility that the assay was not able to detect glutamine in the presence of high glutamate concentrations. This low concentration may indicate that glutamine is rapidly metabolized by SKOV-3 cells and does not accumulate in a steady-state pool needed for this assay method. A method using tracers,

such as flux analysis, would be needed to observe the rapid metabolism of glutamine.<sup>9</sup>

The assays enabled detection of extracellular metabolites in cell culture medium. Only a small volume of medium was needed to measure the four metabolites, allowing the sampling of medium from the same set of wells over time. Although concentrations of each metabolite changed more than 50-fold during 72 h, all measurements were conveniently made with a single dilution factor. Again, we observed differences in OVCAR-3 and SKOV-3 cells with respect to glutamine metabolism, with OVCAR-3 cells secreting much less glutamate over time than the SKOV-3 cells (**Fig. 3D**).

The homogeneous assay format was developed for measuring total lactate or total glutamate directly in the well containing cells. The assays were conducted in LV, 384-well plates and had  $Z'$  values acceptable for HTS. To make the assay HTS compatible, we conducted experiments using cells in suspension. Cells were collected, washed, plated, and pretreated with compounds before medium containing glucose and glutamine was added. Although all sample preparation steps have the potential to change cell metabolism, dispensing prewashed cells in metabolite-free medium allows the compounds to have a greater effect, making the assays more robust and better suited for inhibitor screening.

At the end of the experiment, an acid-lysis strategy was used to quickly lyse cells and inactivate endogenous enzymes with a single addition. Low pH rather than high pH lysis was chosen so that this step would also degrade endogenous NAD(P)H,<sup>30</sup> reducing background signal. The homogeneous assay format is suitable for studying faster-acting compounds, ones that act within a short time frame of  $<2$  h. After this time,

total lactate and glutamate concentrations in the wells will be outside the linear ranges of the assays. A nonhomogeneous format can be used when testing slower-acting compounds, which require longer treatment times.

The lactate and glutamate homogeneous assays were used to screen the LOPAC set of compounds with SKOV-3 cells. We observed decreases and increases in signal for both assays, identifying potential inhibitors and activators of lactate and glutamate production. The metabolite detection assays use coupled enzyme reactions, which can be directly affected by compounds.<sup>31</sup> Therefore, it was important to have a quick, reliable counterscreen to distinguish compounds that interfere with the detection system (false-positive hits) from true-positive hits. For these assays, a counterscreen was readily done using lactate and glutamate controls. Of the most potent hits selected for further study, five of the lactate hits were found to directly and strongly affect the detection system, and one of the glutamate hits was found to have some effect.

Less potent compounds (those with activity between 25%–50% and 125%–150%) were not further analyzed in this study but are also of interest. In addition, monitoring these less potent compounds over longer treatment times could potentially reveal more complex interactions between signaling and metabolic pathways.

The two model ovarian cancer cell lines in this study showed dramatic differences in their glutamine metabolism. Only the SKOV-3 cells were used for screening, but given the differences in their glutamine metabolism, it will be especially interesting to expose the OVCAR-3 cells to the glutamine production activators. Other cancer cell types also exhibit subtype or grade-specific differences,<sup>9,27,28</sup> making it interesting and perhaps even necessary to study more than one cell line. The cell-based bioluminescent assays are suitable for higher-throughput applications and make screening a library with more than one cell line feasible. In this study, the developed protocols were used to screen a library of 1280 compounds; however, using the same principles, they can be applied to smaller and larger screening campaigns.

### Acknowledgments

The authors thank the members of the Promega metabolite detection assay project team for their technical support.

### Declaration of Conflicting Interests

The authors declared the following potential conflicts of interest with respect to the research, authorship, and/or publication of this article: The authors are employees of Promega Corporation.

### Funding

The authors received no financial support for the research, authorship, and/or publication of this article.

### References

1. DeBerardinis, R. J.; Lum, J. J.; Hatzivassiliou, G.; et al. The Biology of Cancer: Metabolic Reprogramming Fuels Cell Growth and Proliferation. *Cell Metab.* **2008**, *7*, 11–20.
2. Pelicano, H.; Martin, D. S.; Xu, R. H.; et al. Glycolysis Inhibition for Cancer Treatment. *Oncogene* **2006**, *25*, 4633–4646.
3. Pusapati, R. V.; Daemen, A.; Wilson, C.; et al. mTORC1-Dependent Metabolic Reprogramming Underlies Escape from Glycolysis Addiction in Cancer Cells. *Cancer Cell* **2016**, *29*, 548–562.
4. Doherty, J. R.; Cleveland, J. L. Targeting Lactate Metabolism for Cancer Therapeutics. *J. Clin. Invest.* **2013**, *123*, 3685–3692.
5. Hensley, C. T.; Wasti, A. T.; DeBerardinis, R. J. Glutamine and Cancer: Cell Biology, Physiology, and Clinical Opportunities. *J. Clin. Invest.* **2013**, *123*, 3678–3684.
6. Dang, C. V.; Le, A.; Gao, P. MYC-Induced Cancer Cell Metabolism and Therapeutic Opportunities. *Clin. Cancer Res.* **2009**, *15*, 6479–6483.
7. Rajagopalan, K. N.; DeBerardinis, R. J. Role of Glutamine in Cancer: Therapeutic and Imaging Implications. *J. Nucl. Med.* **2011**, *52*, 1005–1008.
8. Johnson, A. T.; Kaufmann, Y. C.; Luo, S.; et al. Effect of Glutamine on Glutathione, IGF-1, and TGF-beta 1. *J. Surg. Res.* **2003**, *111*, 222–228.
9. Yang, L.; Moss, T.; Mangala, L. S.; et al. Metabolic Shifts toward Glutamine Regulate Tumor Growth, Invasion and Bioenergetics in Ovarian Cancer. *Mol. Syst. Biol.* **2014**, *10*, 728.
10. Nicklin, P.; Bergman, P.; Zhang, B.; et al. Bidirectional Transport of Amino Acids Regulates mTOR and Autophagy. *Cell* **2009**, *136*, 521–534.
11. Buller, C. L.; Loberg, R. D.; Fan, M.-H.; et al. A GSK-3/TSC2/mTOR Pathway Regulates Glucose Uptake and GLUT1 Glucose Transporter Expression. *Am. J. Physiol. Cell Physiol.* **2008**, *295*, C836–C843.
12. Gao, P.; Tchernyshyov, I.; Chang, T. C.; et al. c-Myc Suppression of miR-23a/b Enhances Mitochondrial Glutaminase Expression and Glutamine Metabolism. *Nature* **2009**, *458*, 762–765.
13. Wise, D. R.; DeBerardinis, R. J.; Mancuso, A.; et al. Myc Regulates a Transcriptional Program That Stimulates Mitochondrial Glutaminolysis and Leads to Glutamine Addiction. *Proc. Natl. Acad. Sci. U. S. A.* **2008**, *105*, 18782–18787.
14. Chokkathukalam, A.; Kim, D. H.; Barrett, M. P.; et al. Stable Isotope-Labeling Studies in Metabolomics: New Insights into Structure and Dynamics of Metabolic Networks. *Bioanalysis* **2014**, *6*, 511–524.
15. TeSlaa, T.; Teitell, M. A. Techniques to Monitor Glycolysis. *Methods Enzymol.* **2014**, *542*, 91–114.
16. Zhang, J.; Ahn, W. S.; Gameiro, P. A.; et al. 13C Isotope-Assisted Methods for Quantifying Glutamine Metabolism in Cancer Cells. *Methods Enzymol.* **2014**, *542*, 369–389.
17. Weindl, D.; Cordes, T.; Battello, N.; et al. Bridging the Gap between Non-Targeted Stable Isotope Labeling and Metabolic Flux Analysis. *Cancer Metab.* **2016**, *4*, 10.

18. Halama, A.; Guerrouahen, B. S.; Pasquier, J.; et al. Metabolic Signatures Differentiate Ovarian from Colon Cancer Cell Lines. *J. Transl. Med.* **2015**, *13*, 223.
19. Fazzari, J.; Lin, H.; Murphy, C.; et al. Inhibitors of Glutamate Release from Breast Cancer Cells: New Targets for Cancer-Induced Bone-Pain. *Sci. Rep.* **2015**, *5*, 8380.
20. Zhang, J. H.; Chung, T. D.; Oldenburg, K. R. A Simple Statistical Parameter for Use in Evaluation and Validation of High Throughput Screening Assays. *J. Biomol. Screen.* **1999**, *4*, 67–73.
21. Zhou, W.; Leippe, D.; Duellman, S.; et al. Self-Immolative Bioluminogenic Quinone Luciferins for NAD(P)H Assays and Reducing Capacity-Based Cell Viability Assays. *ChemBioChem* **2014**, *15*, 670–675.
22. Vidugiriene, J.; Leippe, D.; Sobol, M.; et al. Bioluminescent Cell-Based NAD(P)/NAD(P)H Assays for Rapid Dinucleotide Measurement and Inhibitor Screening. *Assay Drug Dev. Technol.* **2014**, *12*, 514–526.
23. Zhao, L.; Kroenke, C. D.; Song, J.; et al. Intracellular Water-Specific MR of Microbead-Adherent Cells: The HeLa Cell Intracellular Water Exchange Lifetime. *NMR Biomed.* **2008**, *21*, 159–164.
24. Duellmann, S.; Zhou, W.; Meisenheimer, P.; et al. Bioluminescent, Nonlytic, Real-Time Cell Viability Assay and Use in Inhibitor Screening. *Assay Drug Dev. Technol.* **2015**, *13*, 456–465.
25. Radad, K.; Rausch, W.-D.; Gille, G. Rotenone Induces Cell Death in Primary Dopaminergic Culture by Increasing ROS Production and Inhibiting Mitochondrial Respiration. *Neurochem. Int.* **2006**, *49*, 379–386.
26. Wettersten, H. I.; Hakai, A. A.; Morin, D. M.; et al. Grade-Dependent Metabolic Reprogramming in Kidney Cancer Revealed by Combined Proteomics and Metabolomics Analysis. *Cancer Res.* **2015**, *75*, 2541–2552.
27. Gross, M. I.; Demo, S. D.; Dennison, J. B.; et al. Antitumor Activity of the Glutaminase Inhibitor CB-839 in Triple-Negative Breast Cancer. *Mol. Cancer Ther.* **2014**, *13*, 890–901.
28. Wang, G.; Han, T.; Nijhawan, D.; et al. P7C3 Neuroprotective Chemicals Function by Activating the Rate-Limiting Enzyme in NAD Salvage. *Cell* **2014**, *158*, 1324–1334.
29. Coloff, J. L.; Murphy, J. P.; Braun, C. R.; et al. Differential Glutamate Metabolism in Proliferating and Quiescent Mammary Epithelial Cells. *Cell Metab.* **2016**, *23*, 867–880.
30. Lowry, O. H.; Passonneau, J. V.; Rock, M. K. The Stability of Pyrimidine Nucleotides. *J. Biol. Chem.* **1961**, *236*, 2756–2759.
31. Davis, M. I.; Shen, M.; Simeonov, A.; et al. Diaphorase Coupling Protocols for Red-Shifting Dehydrogenase Assays. *Assay Drug Dev. Technol.* **2016**, *14*, 207–212.